International Journal of Engine Research
XX(X):1–12(Author Version)

DOI: 10.1177/14680874211013268
www.sagepub.com/
SAGE

Experimental assessment of ignition characteristics of lubricating oil sprays related to low-speed pre-ignition (LSPI)

Bernardo Tormos[1], José M. García-Oliver[1], Marcos Carreres[1], Carlos Moreno-Montagud[1], Beatriz Domínguez[2], María Dolores Cárdenas[2] and Fermín Oliva[2]

Abstract

Low-speed pre-ignition (LSPI) remains one of the challenges of Direct Injection (DI) Spark Ignition (SI) engines due to its potential to induce a heavy knock. Several mechanisms have been identified in the literature as plausible causes for LSPI. The physical and chemical properties of lubricant oils play a role on some of these causes. The present work aims at getting an independent procedure to determine the proneness of lubricant oils to ignite. To this end, the ignition delay (ID) of different oil formulations is experimentally determined in a constant-pressure flow facility through two different optical techniques: Schlieren and OH* chemiluminiscence imaging. The investigation explores the effect of base-stock formulation, oil specification quality level, different additive types content, aging and oxidation on oil reactivity for several thermodynamic conditions. Differences in ignition delay were found among base stocks, correlating with the American Petroleum Institute (API) group classification. However, no significant differences were found among additive packages previously reported to yield different LSPI occurrences. Hence, oil reactivity does not seem to be a determining factor in this complex phenomenon. Similarly, specific lubricant additive content, aging and oxidation do not importantly modify the measured ignition delay.

Keywords

Low-speed Pre-ignition, Stochastic pre-ignition, Super-knock, Lubricant, Reactivity

1 Introduction

In order to meet the ever more stringent regulations on fuel consumption and emissions, downsizing has become a trend in Direct Injection (DI) Spark Ignition (SI) engines[1,2]. The associated loss in power has had to be compensated by increasing the air intake pressure through turbocharging[3]. As a result, operating in the low-speed and high-load regime has been found to cause the pre-ignition of the flame front. This phenomenon is known as low-speed pre-ignition (LSPI) or stochastic pre-ignition (SPI). These pre-ignitions may in turn lead either to super-knock, heavy-knock, slight-knock or non-knock, most of them leading to a direct damage of the engine[4–6].

As a consequence, researchers have focused on describing mechanisms causing LSPI[7–11], in order to reduce its occurrences through design. The most likely causes for this phenomenon include lubricating oil droplets or solid deposits released in the combustion chamber, either being a source for pre-ignition or acting as a hot spot locally increasing the air-fuel mixture temperature[12]. The pre-ignition leading to super-knock seems to be characterized by a deflagration to detonation transition[13–15]. Through visualization in an optical engine, Feng et al.[16] recently showed that the high-frequency oscillation typical of high knock intensities occurred with the end-gas auto-ignition taking place either close to the pre-ignited flame front or near the cylinder wall.

Even though a universal explanation for the cause of LSPI has not been established yet, several features have been found to influence it. On the one hand, engine hardware and operating conditions play a key role on LSPI. Hence, the use of Exhaust Gas Recirculation (EGR) has demonstrated to reduce its frequency[17–19]. The injection strategy[20–24] may also influence LSPI, the presence of spray-wall interaction[9,25,26] increasing its likelihood.

On the other hand, external to the engine itself, fuel and lubricating oil may promote or mitigate LSPI. Low aromatic content has been reported to reduce pre-ignitions[27,28]. Lean mixture control strategies can also help reducing this problem[29]. Some authors correlated the flame speed variations by fuel type with LSPI[26]. Composition of the lubricant oil also plays an important role. Most researchers have reported an influence of the additive package and detergents[11,30–37], usually implying Ca and Na promoting LSPI with ZDDP (through P) and Mo mitigating it. Nevertheless, Haas et al.[38] observed no statistically significant effect of calcium and magnesium on the Derived Cetane Number (DCN) of lubricating oils through measurements in an Ignition Quality Tester (IQT). Effects of the lubricant oil base stock have also been reported[30,38,39]. An explanation is that some oil components may generate solid deposits and flakes that could act as hot

[1]CMT-Motores Térmicos - Universitat Politècnica de València, Spain
[2]Repsol SA, Spain

Corresponding author:
Marcos Carreres, CMT-Motores Térmicos Universitat Politècnica de València, Camino de Vera s/n, Valencia, 46022, Spain.
Email: marcarta@mot.upv.es

spots[40]. However, Ohtomo et al.[41] demonstrated in a rapid compression expansion machine (RCEM) that an oil droplet itself could be responsible for LSPI if it remained in the chamber over the exhaust stroke, staying hot in the next cycle. In this sense, Ullal et al.[42] have recently shown the importance of the oil drop residence time on its pre-ignition through a numerical investigation. Finally, Hirano et al.[31] investigated the effect of used and degraded oils, reporting they may increase the LSPI frequency but obtaining varied results depending on the baseline oil studied.

Most of the studies reported were conducted in an engine, making it difficult to isolate the driving mechanisms from engine-dependent effects. Evidences that lubricating oil may be a trigger to LSPI should be independently evaluated, in such a way that an independent test procedure could be established to determine oil tendency to LSPI. In the present investigation, lubricant oil ignition delay (ID) is measured for different thermodynamic conditions by spraying it into a constant-pressure flow facility and visualizing it through two different optical techniques, namely Schlieren and OH* chemiluminiscence imaging. Different oil lubricant formulations are studied, including base stocks ranging all groups from the American Petroleum Institute (API) categorization[43]. The effect of the additive package on oil reactivity is also studied, including formulations that are claimed to induce lower LSPI occurrences than others. This allows validating if the measured oil reactivity trends agree with reported LSPI data. For a given base stock and additive package formulation, the influence of aging and oxidation is also assessed. Finally, substances with different additive types content (anti-wear, anti-oxidants and friction modifiers) are analyzed, too.

The objective of the work is to determine whether the propensity of a a given oil formulation to induce LSPI can be assessed independently from an engine test. If this was the case, the proposed methodology could be used as a simpler tool for lubricant formulation benchmarking than the Sequence IX Test[44] or other currently widespread engine tests. Otherwise, the implication would be that the differences in reactivity among lubricating oils are not the explaining factor for their different LSPI occurrences in an engine.

2 Materials and methods

2.1 Constant-pressure flow facility

All the experiments to determine the ID of the different lubricating oils have been carried out in a high temperature and high pressure test chamber that allows reproducing relevant in-cylinder thermodynamic conditoins to study fuel or lubricating oil injection, evaporation and combustion. The facility procures keeping these conditions nearly quiescent and steady, obtaining a low shot-to-shot dispersion[45]. According to the convention presented by Baert et al.[46], this test rig is classified as a constant-pressure flow facility, since the high pressure high temperature gas continuously flows through the chamber. For a thorough description of the facility, the reader may refer to other works[45,47].

Gas flow and its corresponding pressure are ensured thanks to air compressors, N_2 and O_2 bottles whose flow is conditioned through control valves. The gas temperature is achieved in the chamber thanks to a set of electrical resistors placed in the incoming gas inlet pipe. This arrangement allows keeping a maximum temperature of 1000 K and a maximum pressure of 15 MPa. Temperature is monitored by means of a series of type-K thermocouples with an estimated accuracy of ± 3 K, whereas a Wika S-20 pressure sensor with an estimated accuracy of $\pm 0.5\%$ is placed in the internal wall of the chamber. Optical access to the test rig is gained through three circular optical accesses (128 mm in diameter), as shown in Figure 1.

2.2 Injection system

Each lubricating oil was sprayed into the test rig through an adapted common-rail system, comprising a Nova Swiss high-pressure pneumatic pump driven by an electric motor, a common-rail with pressure regulation controlled by a PID and a Bosch solenoid injector.

A single-hole axial nozzle with a convergent shape (orifice outlet diameter of 112 μm) was adapted to the injector in order to simplify the visualization process focusing on a single spray. The geometrical and flow features of this nozzle are well-known from previous experimental studies concerning internal nozzle flow[48] and spray behaviour[49–51].

Long injector energizing times (ET) were adopted (see Section 2.3) so that the ignition took place while oil was still being sprayed into the chamber, in order to isolate the chemical effects on the ID from the physical ones (please note that Kuti et al.[52] already reported the chemical ID playing a greater role than the physical ID in the differences among substances). Similarly, a relatively high injection pressure $p_i = 100$ MPa was chosen for all tests so as to obtain an efficient atomization in order to remove the influence from the physics, while keeping the ignited spray within the optical window.

2.3 Test matrix

The thermodynamic conditions provided by the chamber in the tests are shown in Table 1. Two different chamber pressures were chosen in order to study the effect of air density at each temperature tested. For each ambient condition and substance tested, 10 injections were recorded in order to provide statistically reliable data, with an injection frequency of 0.25 Hz.

Table 1. Operating conditions tested in the constant-pressure flow facility.

Temperature T [K]	Backpressure p_b [MPa]	Gas density ρ_g [kg/m^3]	Energizing Time ET [ms]
750	5	22.8	2
	7.5	33.9	2
775	5	22.1	2
	7.5	32.8	2
800	5	21.4	1
	7.5	31.8	1
850	5	20.1	1
	7.5	29.9	1

It is important to note that the chosen test matrix partly aims at reproducing engine-like operating conditions.

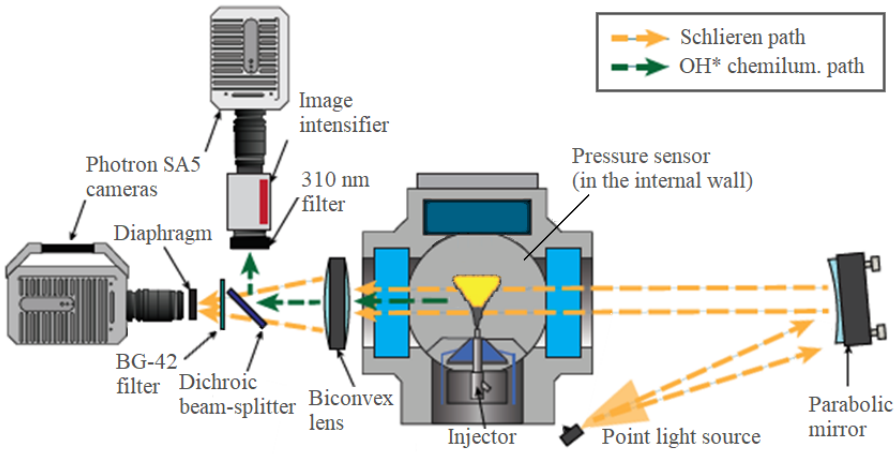

Figure 1. Top view of the experimental facility and optical setup.

While most tested temperatures are representative of Top Dead Centre (TDC) in-cylinder values reached within GDI engines, the chamber pressures (and the associated densities) needed to be relatively high in order for the spray to ignite within the range of the test rig optical access. Please note that typical compression ratios among 9.5 and 11.5 lead to chamber pressures around 4 to 5.5 MPa. Hence, the tested conditions that fall out of the usual range of operation of GDI engines ($p_b = 7.5$ MPa and $T = 850$ K) are expected to increase oil reactivity in the constant-pressure test rig.

The different lubricating oils tested to study the effect of the base stock formulation and additive package on the ID are shown in Table 2. Oils #1 to #6 were chosen to study the influence of the base stock considering the same additive package, whereas oil #3 together with oils #7 to #9 were chosen to study the influence of the additive package for the same base stock. Hence, oil #3 is the substance defined as a common reference in both comparisons. Base stock formulations are classified according to the API categorization[43]. Furthermore, an extra formulation has been considered using a base stock G-III+: even if this is not a base oil category but rather a marketing term used to define higher viscosity index (VI) base stocks, a broad usage of this stock in high performance lubricants is expected for the automotive sector. Finally, G-V base stock is an ester that falls outside the previous categories.

Table 2. Lubricating oil formulations tested to determine the influence of the base stock and the additive package on the ID. The substance taken as a reference is highlighted in bold.

Oil #	Base stock	Additive package
1	Group-I	**API SN Plus (Supplier I)**
2	Group-II	
3 (ref)	**Group-III**	
4	Group-III+	
5	Group-IV	
6	Group-V (Ester)	
7	Group-III	ACEA C5
8		API SN
9		API SN Plus (Supplier II)

For the additive packages, the specification quality level reached by each formulation and the supplier of the package has been used as a differential parameter. Hence, either the API[53] or the ACEA (European Automobile Manufacturer's Association) European Oil Sequences[54] have been used as specification references. API SN Plus is a supplemental oil category from API for those oil formulations specifically designed to help prevent LSPI in GDI engines and consequently it represents an improvement on API SN formulations.

In order to assess the specific effect of some type of additives inside the general additive package, some variations of the original version of Oils #3 and #9 with higher levels of anti-wear, anti-oxidant and friction modifiers have been tested. Finally, the effects of oil aging and oxidation have been assessed after forcing those events for both Oils #3 and #1. Each oil sample has been aged on a real engine for 100 hours of usage under a specific working cycle. Oxidized samples have been obtained through a typical oxidation lab procedure whose main characteristics are as follows: operation temperature of 443 K, air flow rate of 60 L/h, 100 ppm of Fe as a catalytic metal during 144 h. The codes to identify these additional substances are summarized in Table 3, making up for a total of 19 lubricating oils tested.

Table 3. Additional versions of lubricating oil formulations tested to determine the influence of the additive types content, aging and oxidation.

Oil #	Anti-wear	Anti-oxid.	Frict. mod.	Aged	Oxidized
1	-	-	-	1.A	1.O
3	3.AW	3.AO	3.FM	3.A	3.O
9	9.AW	9.AO	9.FM	-	-

The contribution of two of the most remarkable elements to the composition of the additivation packages is shown in Table 4 for reference. Please also note that all of them present a similar content of ZDDP. Table 4 reflects that the claimed better performance against LSPI of the API SN PLUS variant when compared to the API SN is achieved by reducing the calcium content and compensating the detergency properties with an increase in magnesium. No significant difference in this terms is noted among the different additive package variations tested, even though the addition of Mg by Supplier II is less important.

Table 4. Content (in ppm) of some metals in the oil additive packages tested.

Additive package	Ca	Mg
API SN	2222	8
ACEA C5	1737	11
API SN Plus S.I	1246	810
API SN Plus S.II	1229	537
API SN Plus S.I, AW	1288	805
API SN Plus S.I, AO	1194	763
API SN Plus S.I, FM	1280	795

2.4 Optical techniques and setup

As shown in Figure 1, two different optical techniques were simultaneously used to determine the ID of the lubricating oils through spray visualization, namely Schlieren and chemiluminiscence of OH* radicals. The arrangement is similar to the one successfully used by Payri et al.[55] to determine the ID of Diesel fuel sprays and single component surrogates. Similar arrangements have also been used by other authors to determine ID and lift-off length[56] in the frame of the Engine Combustion Network (ECN)[57].

2.4.1 Schlieren imaging with background lighting Schlieren imaging allows identifying gradients in the refractive index of transparent mediums. This technique has been widely utilized to capture the boundary between vaporized fuel and ambient gas in Diesel sprays[58,59]. Benajes et al.[60] have also used this technique in the described facility to quantify the ignition delays of this type of sprays.

The path for the light beam used for the single-pass Schlieren setup is shown in Figure 1. A Xe-arc light source (1000 W) is pointed towards a parabolic mirror, which collimates the rays generating a cylindrical beam travelling through the test rig. A biconvex lens collects the parallel light rays and converges them to the image focus (650 mm) where they are captured by a Photron SA-5 fast camera after being filtered by a BG-42 filter, which helps reducing the effect of strong soot radiation on the Schlieren signal. Any beam deflections generated in the test chamber by gradients in the refractive index are visualized as shades in the images. The camera settings are summarized in Table 5.

Table 5. Summary of the Photron SA-5 camera settings used for each technique.

Setting	Schlieren	OH* chemiluminiscence
Frame rate (fps)	30000	75000
Shutter speed (μs)	6.5	4.2 to 18.1
Image size (px)	320x616	320x408
px/mm	6.85	4.15

2.4.2 Chemiluminiscence of OH radicals* The start of ignition of the oils was also estimated through the detection of OH* radicals chemiluminiscence. The use of this signature to determine ID was first introduced and validated by Lillo et al.[61] and has already been used in the facility described in the present work[60].

As seen in Figure 1, in this case the signal comes directly from light emissions in the chamber. After leaving the test rig and trespassing the biconvex lens, the emission is deflected by a dichroic beam-splitter and acquired by another Photron SA-5 fast camera. This camera is fitted with a 310 nm interference filter, to reject all wavelengths except the one corresponding to the peak emission of OH* radicals. Given that the resultant signal is weak, the intensifier of the camera sensor was gated during the steady part of the injection. The settings of this second camera are also summarized in Table 5.

2.5 Image processing

A sample of images obtained through both techniques and different operating conditions is shown in Figure 2.

Let us consider the images obtained through Schlieren and OH* chemiluminiscence for $T = 850$ K as a reference to explain the ignition sequence. The SOI (Start of Injection) occurs slightly earlier than $t_{aSOE} = 367$ μs. The spray penetrates into the chamber ($t_{aSOE} = 700$ μs) until the side of the spray partially disappears from the Schlieren image ($t_{aSOE} = 767$ μs). This event corresponds to the Start of Cool Flames (SCF) stage reported in the literature[60]. Pickett et al.[62] observed this stage as a temporal disappearance of the spray in the tip region, which may also be appreciated at $t_{aSOE} = 800$ μs in Figure 2 (center). Along this stage low temperature reactions are taking place, which slightly increases temperature and hence softens density gradients, explaining why the spray tip becomes 'transparent' before the start of high temperature reactions or Second Stage Ignition (SSI). The spray tip then reappears in the Schlieren images and is observed as an expanded spray. Also at this instant (already developed at $t_{aSOE} = 900$ μs for the Schlieren sequence), bright points appear in the OH* chemiluminiscence signal detected, as appreciated among $t_{aSOE} = 827$ μs and $t_{aSOE} = 853$ μs. This instant is the reference for the ID in the present work. In subsequent frames, the spray front is seen to produce strong radiation, which mostly stems from soot production by the lubricating oil combustion ($t_{aSOE} = 1067$ μs). Later on, the OH* chemiluminiscence signal is detected along the spray ($t_{aSOE} = 2520$ μs) Finally, the injection stops and combustion is extinguished close to the spray tip, although some remaining oil droplets seem to generate soot in the Schlieren image ($t_{aSOE} = 3500$ μs).

These sequences are consistent with the ones described by other authors[63,64] for reacting Diesel jets. In fact, Skeen et al.[63] already pointed out the partial disappearence of some regions at the side of the spray prior to the temporal disappearance of the spray tip. Figure 2 (left) highlights the importance of this fact, since it demonstrates that, in the case of the lubricating oil, at low temperatures ($T <= 800$ K) the SCF stage can only be noted in the shown frames through the side of the spray, no difference in the spray tip being appreciated in the temporal window shown.

The images are processed using in-house codes programmed in Matlab to obtain the ID. In order to remove the influence of injector dynamics (i.e. physics) in the computed ID values, the Start of Injection (SOI) is used as the temporal origin rather than the Start of Energizing (SOE). The SOI is estimated by linearly fitting the temporal evolution of the spray penetration and extrapolating the resultant fit to the instant of null penetration.

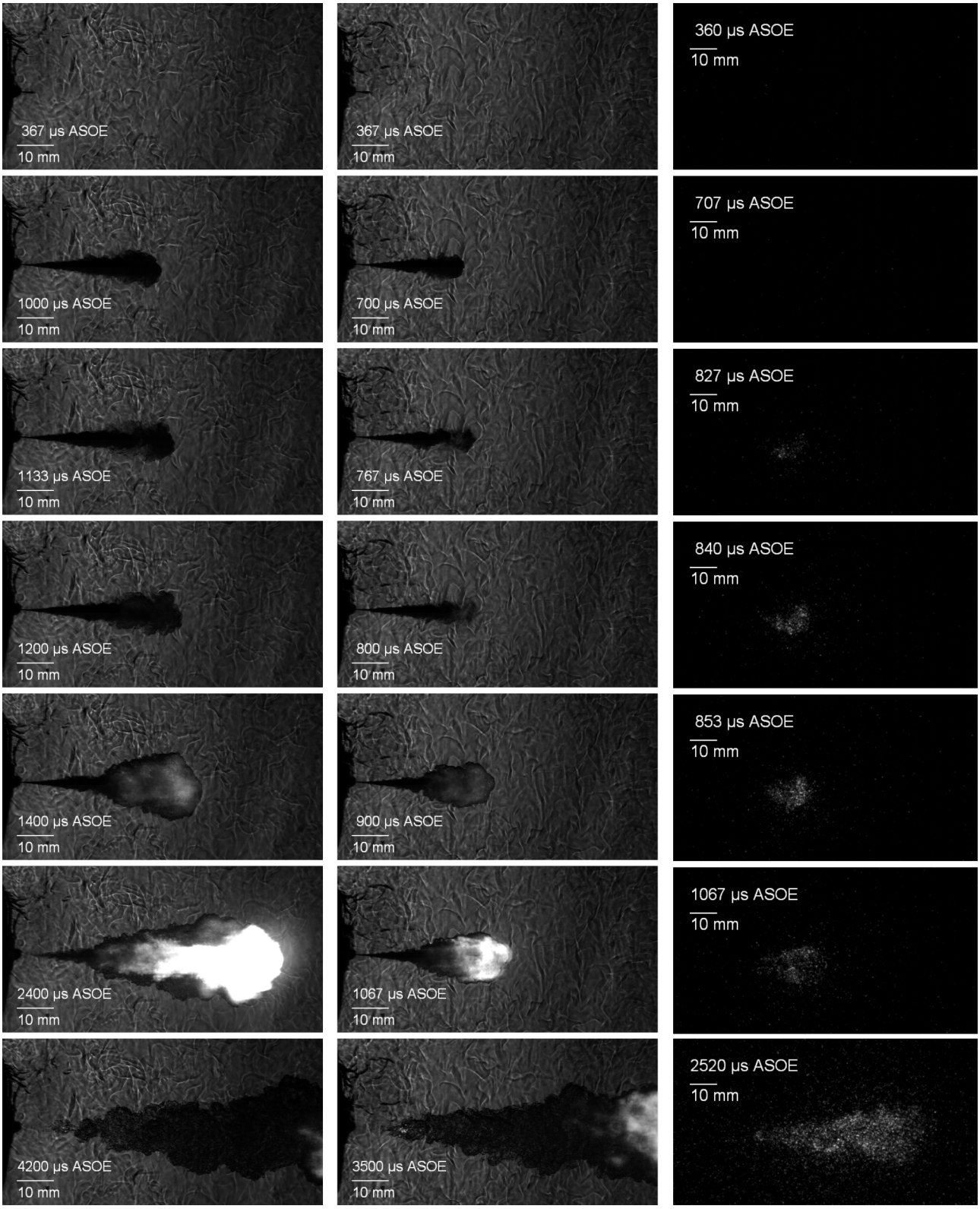

Figure 2. Images displaying the sequence of ignition for the oil #3 at $p_b = 5$ MPa (left: Schlieren technique, $T = 800$ K; center: Schlieren technique, $T = 850$ K; right: Chemiluminiscence of OH* radicals, $T = 850$ K). All times ASOE (after start of energizing).

Figure 3 compares the evolution of the spray penetration (normalized with the equivalent nozzle diameter, i.e. outlet diameter times square root of the density ratio) for oil #3 at $T = 800$ K (matching the sequence from Figure 2) and the ECN Spray A available data[57] to illustrate the similarities among the lubricating oils injection and well-known Diesel-like sprays. Despite the differences in ambient temperature and pressure, liquid properties and injection setup, the normalized curves are very similar. This fact highlights that the spray generated with lubricating oils by a single-hole nozzle can be studied through the same techniques widely used to study the Diesel injection process.

The criteria to determine the ID for the two optical techniques used are explained next.

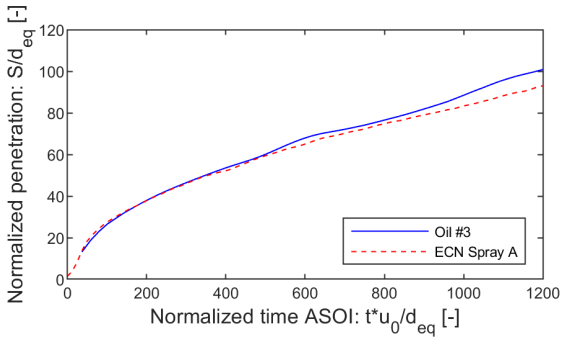

Figure 3. Temporal evolution of the spray penetration for Oil #3 at $T = 800$ K and $p_b = 5$ MPa ($p_i = 100$ MPa, $ET = 1$ ms) and the ECN Spray A data[57] (the Spray A operating condition responds to a single-hole nozzle operated with n-dodecane for $T = 900$ K and $p_b \approx 6$ MPa, with $p_i = 150$ MPa and $ET = 2$ ms). Time normalized with the injection velocity and the equivalent diameter; penetration normalized with the equivalent diameter (where the equivalent diameter is the nozzle outlet diameter times the square root of the fuel-to-air density ratio.)

2.5.1 Schlieren imaging The ID has been determined from the images as the instant at which the spray expansion takes place. To compute this instant, the spray contour needs first to be detected for all frames of a given test repetition. The methodology for contour detection includes a dynamic-background substraction and composition to remove the influence of the background and an image binarization. The latter has been performed as proposed by Siebers[65], using a set level of the dynamic range between 5%-8% for all tested conditions. A thorough description of the contour detection procedure may be found elsewhere[66].

Once the spray contour is detected, the number of pixels within the spray is computed for each frame (see Figure 4). At the time of spray expansion, the number of pixels grows importantly. This instant is characterized by the temporal evolution of the time derivative of the spray pixel count, also shown in Figure 4. The ID for a given substance and operating condition is then determined as the average instant at which the maximum of the spray pixel derivative is found for the 10 repetitions tested.

2.5.2 OH chemiluminiscence signal* In the case of the OH* chemiluminiscence images, the addition of the intensity luminosity of all pixels is computed for each frame. Once the temporal evolution of the intensity signal is obtained (see Figure 4), an important increase is observed by the time of ignition. A threshold level is used to remove the influence of the background signal and compute the ID, which is averaged for the 10 repetitions tested.

3 Results and discussion

In this Section, a comparison among the results obtained with both experimental techniques is first shown. Next, the actual study of the lubricant oil reactivity is performed, analyzing the influence of the base stock, the additive package and its modifiers, aging and oxidation.

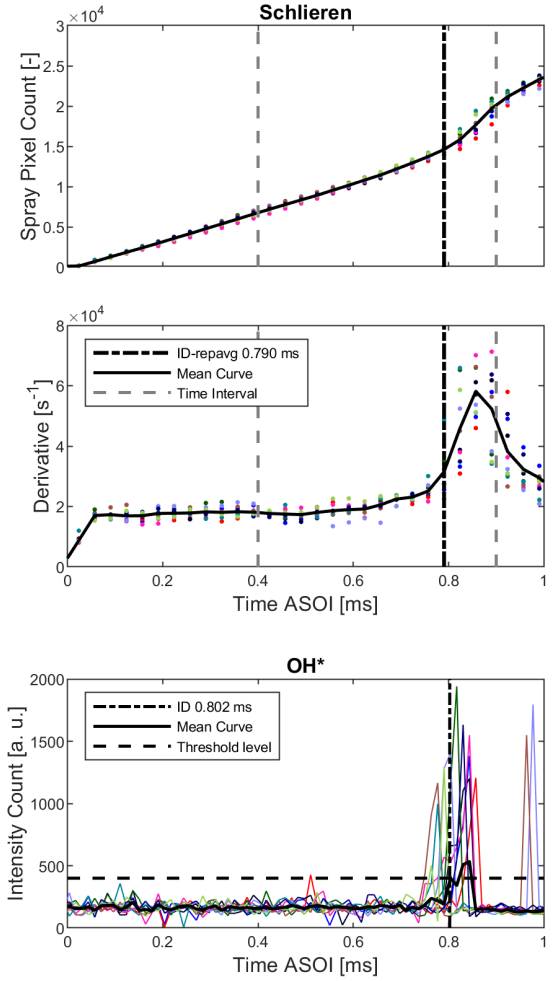

Figure 4. Temporal evolution of the signals used to determine the ID through Schlieren (spray pixel count and its derivative, top) and OH* chemiluminiscence (intensity count, bottom). Oil #3, $T = 800$ K, $p_b = 5$ MPa, $p_i = 100$ MPa, $ET = 1$ ms.

3.1 Comparison of optical techniques

Figure 5 shows the comparison among the ID results obtained through the Schlieren imaging and OH* chemiluminiscence techniques for all the operating conditions tested for a given lubricating oil.

Mean results show that both techniques estimate a similar ID for all tested points, regardless of the operating conditions tested. In the cases where slight deviations are found among techniques, they could not be related to the effect of a particular operating condition, meaning that both techniques allow accurately determining the ID trends with pressure and temperature. The standard deviation of the measurements is generally low for both techniques. Nevertheless, they are generally lower and more consistent among operating conditions for the OH* chemiluminiscence. For this reason, results obtained through this technique will be used as a basis for the rest of the analysis.

3.2 Influence of the base stock on the lubricant oil reactivity

The results obtained for Oil #1 to Oil #6 (recall Table 2) to analyze the influence of the base stock formulations on reactivity are shown in Figure 6. Results are plotted as a

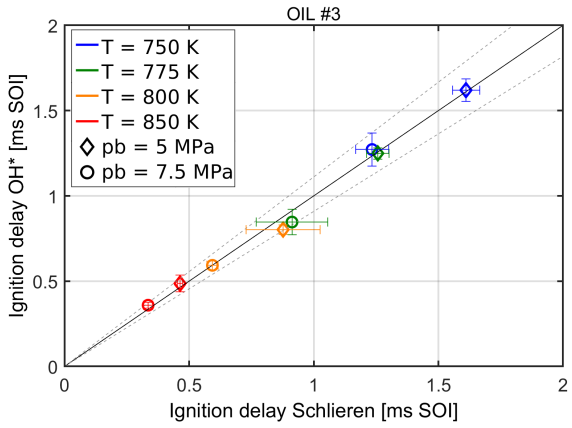

Figure 5. ID results comparison among techniques. Lines coming out from the symbols represent the standard deviation among repetitions. The dashed lines represent a 10% deviation among techniques. Oil #3.

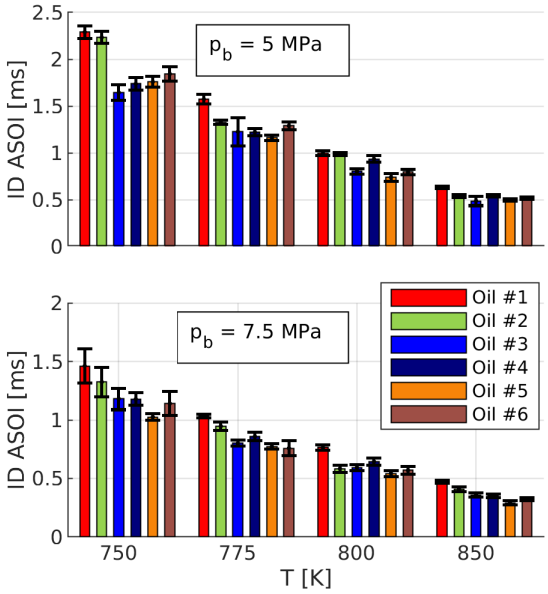

Figure 6. ID trends with T and p_b obtained through OH* chemiluminiscence for lubricating oils with different base stock formulations and the API SN Plus (Supplier I) additive package.

function of chamber temperature and pressure. As expected, for a given substance the ID decreases (i.e. reactivity increases) with increasing temperature and pressure. Above $T = 800$ K, no significant differences are observed among base stock formulations, except for Oil #1 (base stock Group I). At lower temperatures (and especially low pressure), Oil #1 and Oil #2 (Group II) showed less reactivity than the rest. This result is in agreement with the investigations carried out by Takeuchi et al.[30] in an engine and Haas et al.[38] in an Ignition Quality Tester (IQT), where reactivity was found to increase with increasing API Group number. Since lubricating oils are composed of paraffinic components, without aromatics, Haas et al. attributed this trend to the increasing methylene (CH_2) to methyl (CH_3) ratio in the ^{1}H NMR spectrum of these substances with increasing group number. Hence, this result is consistent with the fuel ignition propensity being correlated by the ratio of CH_2 and CH_3 as found by Won et al.[67]. Oil #5 (ester, labelled as Group V) escapes from the trend given its specific nature. In any case, this result implies that, if oil reactivity importantly drove LSPI, base stock formulations with generally attributed lower quality might be beneficial for this particular issue.

3.3 *Influence of the additive package on the lubricant oil reactivity*

The comparison among Oil #3 and Oils #7 to #9 is shown in Figure 7. No significant differences are observed among oils for $T \geq 775$ K. Focusing on the $T = 750$ K results, the differences observed among suppliers (Oils #3 and #9) are not fully coherent among pressures. In any case, Oils #7 (ACEA C5 additive package) and #8 (API SN additive package) are found to present a higher ID (i.e. less reactivity) than Oils #3 and #9 (API SN Plus additive packages) for the low pressure case representative of engine conditions. This fact is not aligned with the API SN Plus reducing LSPI occurrences in standard LSPI engine tests. As seen in Table 4, the most significant differences among these additive packages are found in the Ca and Mg content. Oils #7 and #8 present a higher Ca content, reported to promote LSPI in engine tests in the literature[31,33,34,36], than Oils #3 and #9. The latter compensate the reduction in Ca to reduce LSPI frequency with an addition of Mg, generally found to have no influence on LSPI in engine tests[34,36].

However, in terms of reactivity, the opposite trend to LSPI frequency is found here: oils with more Ca present a lower reactivity. In fact, there is a disagreement among the LSPI occurrences reported in the literature with engine tests and the reactivity results observed through other techniques. Haas et al.[38] reported no significant effects of Ca on the oil reactivity in their IQT tests. Even though Kassai et al.[68] did report a lower ID for calcium-rich oils in a constant-volume chamber (CVC) and a RCM, the oils were blended with fuel: Splitter et al.[69] showed no effect of the oil detergent additives on LSPI when the oil was blended with an LSPI promoter fuel, but they did find an effect of the detergent when they changed the fuel distillation and added spray-wall interaction. Results presented in this work, together with this analysis from the literature, suggest that oil reactivity defined in terms of autoignition propensity does not seem to be a determining factor in LSPI. Hence, LSPI seems to be explained by a combination of several mechanisms, including engine-related factors together with the tendency of an oil droplet to stay in the chamber for the next cycle after the exhaust stroke[41].

3.4 *Influence of different additive types content on the lubricant oil reactivity*

Figure 8 shows the comparison among Oils #3 and #9 with their versions with higher content of specific additive types: anti-wear (AW), anti-oxidants (AO) and friction modifiers (FM), as shown in Table 3. Results show no significant differences among substances for any of the suppliers at any temperature. Where differences are found (i.e. Oil #3 with its different versions at $T = 800$ K or Oil #9.FM with the rest of Oil #9 variations at $T = 800$ K), they are not fully consistent

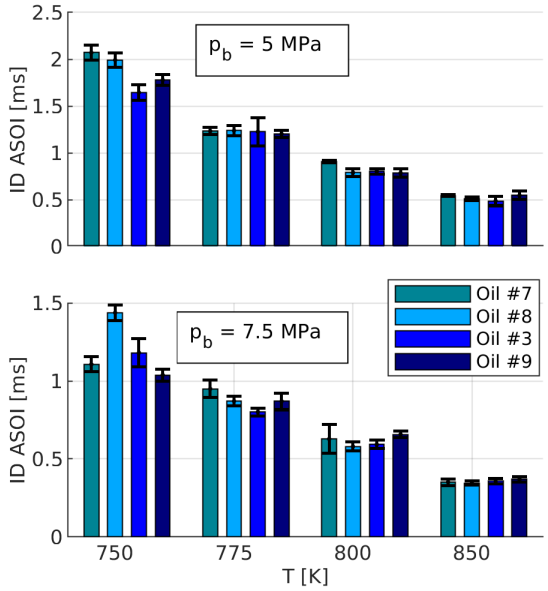

Figure 7. ID trends with T and p_b obtained through OH* chemiluminiscence for lubricating oils with Group III base stock formulation and different additive packages.

among chamber pressures. Hence, no significant influence of different additive types on oil reactivity has been noticed.

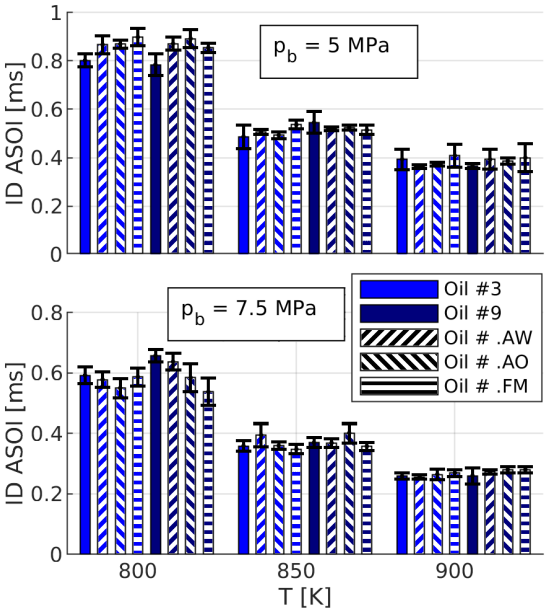

Figure 8. ID trends with T and p_b obtained through OH* chemiluminiscence for lubricating oils with Group III base stock formulation and API SN Plus additive packages from two different suppliers with modifiers.

3.5 Influence of aging and oxidation on the lubricant oil reactivity

Last, it is interesting to determine if lubricant aging or oxidation influence the ID differently depending on the original oil composition, to understand if oil degradation could play a role on oil reactivity. Figure 9 shows the comparison among Oils #1 and #3 with their aged (A) and oxidized (O) versions as shown in Table 3. In the view of the figure, there are significant differences among a given oil and their associated A and O variants (especially the lower the ambient temperature, and more noticeable for Oil #1). Where there are differences, it may be seen that oxidation and especially aging increase the ID (i.e. reduce reactivity) compared to the original formulation. Nevertheless, the trends seen among bases are not modified by oxidation and aging: any version of Oil #1 (API Group I base stock) exhibits a lower reactivity than its corresponding version of Oil #3 (API Group III base stock). It is important to note that Hirano et al.[31] found in engine tests that the used samples of some oils increased LSPI frequency with respect to a new substance, whereas the use in some other formulations did not increase LSPI occurrence. Hence, the reduction in oil reactivity among baseline substances and their aged and oxidized variants does not seem to be the factor explaining LSPI occurrence in an engine.

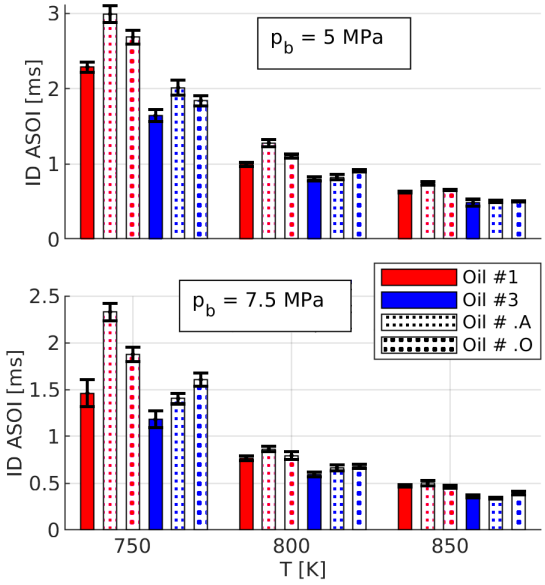

Figure 9. ID trends with T and p_b obtained through OH* chemiluminiscence for aged and oxidized lubricating oils with different base stocks and the API SN Plus (Supplier I) additive package.

4 Limitations of the study

As stated in the Introduction, the objective of the work is to determine whether the propensity of a a given oil formulation to induce LSPI can be assessed independently from an engine test. Since the formulations with the API SN Plus additive package (generally accepted to reduce LSPI occurrence in engine tests) exhibited higher reactivity than API SN and ACEA C5 formulations, it appears the LSPI propensity trends among oil formulations cannot be solely explained by the differences in reactivity exhibited in a constant-pressure flow chamber. Hence, the findings in these tests cannot be extrapolated to an engine environment.

The explanation should reside in the fact that the LSPI occurrence involves several mechanisms interacting in the

engine, which cannot be fully simulated in a constant-pressure or a constant volume flow chamber. An important shortcoming of the technique is that the measurements are taken on single isolated cycles. As stated in the Introduction, one factor triggering LSPI occurrence may be the formation of solid deposits and flakes along several cycles, acting as hot spots on a given random cycle. These particles can come from the combustion chamber walls themselves or from lubricant additives generated along the cycles (for instance, CaO formation) that absorb CO_2 in subsequent cycles with evolving heat, causing pre-ignition[40]. Other factors that cannot be recreated in the test rig are surface ignition or the impact of residual gases[7].

Therefore, explanations for LSPI occurrence and its trends in an engine seem to require the combination of engine-related, oil-related and fuel-related mechanisms interacting with each other, hardly replicable in a constant-pressure flow chamber. In any case, the exercise on oil ignition characteristics carried out in the present investigation contributes to this understanding.

5 Conclusions

The ignition delay (ID) of lubricating oils with several formulations has been experimentally determined for several engine-related ambient conditions through two different optical techniques in order to understand the role of oil reactivity on LSPI. Experiments were conducted in a constant-pressure flow facility in order to understand if a LSPI test could be established independently from an engine. The main findings of the work are summarized as follows:

- Schlieren and chemiluminiscence of OH* radicals are both suitable to determine the ID of relatively reacting substances. No significant differences have been observed among techniques, although a more consistent repeatability has been observed for the latter.
- Oil reactivity has been found to increase with increasing base stock API Group number (except for Group V, which falls out from the categorization), in agreement with recent results from the literature that attributed this fact to the methylene (CH_2) to methyl (CH_3) ratio in the formulations.
- Despite their lower Ca content, formulations with the API SN Plus additive package generally known to reduce LSPI occurrence in engine tests exhibited higher reactivity than API SN and ACEA C5 standard formulations. Experimental works in IQT or RCEM in the literature already reported no significant differences in oil reactivity among formulations with low Ca content, in agreement with the measurements presented in this work.
- Anti-wear, anti-oxidation and anti-friction additive package modifiers do not significantly influence lubricant oil reactivity.
- Oil oxidation and aging reduce reactivity compared to the original oil formulations, which would in fact mitigate LSPI if oil reactivity was a relevant factor. In any case, the trends among oil formulations were not found to be modified by oxidation and aging.

From the aforementioned conclusions, it follows that the differences in reactivity (defined in terms of autoignition propensity) among lubricating oils are not the factor explaining their different LSPI occurrences in an engine. LSPI should then be explained by a combination of engine-related, oil-related (including reactivity) and fuel-related mechanisms interacting in an engine. The present investigation shows that these mechanisms could not be simulated in constant-presure or constant-volume vessels to extrapolate the findings to an engine environment.

Acknowledgements

The authors thank Omar Huerta and Mario Belmar for their technical help during the experimental campaign, laboratory work and data processing.

Declaration of conflicting interests

The authors declare no potential conflicts of interest with respect to the research, authorship and/or publication of this article.

Funding

Part of the experimental hardware used in this work was purchased through funds obtained from IDIFEDER/2018/037 “Diagnóstico óptico a alta velocidad para el estudio de procesos termo-fluidodinámicos en sistemas de inyección”.

References

1. Kalghatgi GT, Bradley D, Andrae J et al. The nature of ”superknock” and its origins in SI engines. *Institution of Mechanical Engineers - Internal Combustion Engines: Performance, Fuel Economy and Emissions* 2009; : 259–269.
2. Kalghatgi GT. Developments in internal combustion engines and implications for combustion science and future transport fuels. *Proceedings of the Combustion Institute* 2015; 35(1): 101–115. DOI:10.1016/j.proci.2014.10.002.
3. Harvey A, Desercey G, Heikal M et al. Low-speed pre-ignition in gasoline, turbo-charged, direct injection engines: An analysis of engine testing data. *AIP Conference Proceedings* 2018; 2035. DOI:10.1063/1.5075580.
4. Zahdeh A, Rothenberger P, Nguyen W et al. Fundamental Approach to Investigate Pre-Ignition in Boosted SI Engines. *SAE International Journal of Engines* 2011; 4(1): 246–273. DOI:10.4271/2011-01-0340.
5. Wang Z, Liu H and Reitz RD. Knocking combustion in spark-ignition engines. *Progress in Energy and Combustion Science* 2017; 61: 78–112. DOI:10.1016/j.pecs.2017.03.004.
6. Wang W, Lu Y, Li Z, and Li H. Simulations of engine knock flow field and wave-induced fatigue of a downsized gasoline engine. *International Journal of Engine Research* 2021; 22(2):554–568. DOI:10.1177/1468087419859791
7. Dahnz C, Han K-M, Spicher U, et al. Investigations on Pre-Ignition in Highly Supercharged SI Engines. *SAE International Journal of Engines* 2010; 3(1): 215–224. DOI:10.4271/2010-01-0355
8. Kalghatgi GT and Bradley D. Pre-ignition and ’super-knock’ in turbo-charged spark-ignition engines. *International Journal of Engine Research* 2012; 13(4): 399–414. DOI:10.1177/1468087411431890.
9. Palaveev S, Magar M, Kubach H et al. Premature flame initiation in a Turbocharged DISI engine - Numerical and

experimental investigations. *SAE International Journal of Engines* 2013; 6(1): 54–66. DOI:10.4271/2013-01-0252.

10. Zaccardi JM and Escudié D. Overview of the main mechanisms triggering low-speed pre-ignition in spark-ignition engines. *International Journal of Engine Research* 2015; 16(2): 152–165. DOI:10.1177/1468087414530965.
11. Kassai M, Torii K, Shiraishi T et al. Research on the Effect of Lubricant Oil and Fuel Properties on LSPI Occurrence in Boosted S. I. Engines. *SAE Technical Papers* 2016; DOI: 10.4271/2016-01-2292.
12. Su J, Dai P and Chen Z. Detonation development from a hot spot in methane/air mixtures: Effects of kinetic models. *International Journal of Engine Research* 2020; (In press). DOI:10.1177/1468087420944617.
13. Wang Z, Qi Y, He X et al. Analysis of pre-ignition to super-knock: Hotspot-induced deflagration to detonation. *Fuel* 2015; 144: 222–227. DOI:10.1016/j.fuel.2014.12.061.
14. Robert A, Richard S, Colin O et al. LES study of deflagration to detonation mechanisms in a downsized spark ignition engine. *Combustion and Flame* 2015; 162(7): 2788–2807. DOI:10.1016/j.combustflame.2015.04.010.
15. Robert A, Zaccardi JM, Dul C et al. Numerical study of auto-ignition propagation modes in toluene reference fuel–air mixtures: Toward a better understanding of abnormal combustion in spark-ignition engines. *International Journal of Engine Research* 2019; 20(7): 734–745. DOI:10.1177/1468087418777664.
16. Feng D, Buresheid K, Zhao H et al. Investigation of lubricant induced pre-ignition and knocking combustion in an optical spark ignition engine. *Proceedings of the Combustion Institute* 2019; 37(4): 4901–4910. DOI:10.1016/j.proci.2018.07.061.
17. Amann M, Alger T and Mehta D. The Effect of EGR on Low-Speed Pre-Ignition in Boosted SI Engines. *SAE International Journal of Engines* 2011; 4(1): 235–245. DOI: 10.4271/2011-01-0339.
18. Gupta A, Seeley R, Shao H et al. Impact of Particle Characteristics and Engine Conditions on Deposit-Induced Pre-Ignition and Superknock in Turbocharged Gasoline Engines. *SAE International Journal of Fuels and Lubricants* 2017; 10(3): 830–841. DOI:10.4271/2017-01-2345.
19. Parsons D, Orchard S, Evans N et al. A comparative study into the effects of pre and post catalyst exhaust gas recirculation on the onset of knock. *International Journal of Engine Research* 2020; (In press). DOI:10.1177/1468087420962294.
20. Wang Z, Qi Y, Liu H et al. Experimental Study on Pre-Ignition and Super-Knock in Gasoline Engine Combustion with Carbon Particle at Elevated Temperatures and Pressures. *SAE Technical Papers* 2015; DOI:10.4271/2015-01-0752.
21. Han L, Zhu T, Qiao H et al. Investigation of Low-Speed Pre-Ignition in Boosted Spark Ignition Engine. *SAE Technical Papers* 2015; DOI:10.4271/2015-01-0751.
22. Mayer M, Hofmann P, Geringer B et al. Influence of Different Oil Properties on Low-Speed Pre-Ignition in Turbocharged Direct Injection Spark Ignition Engines. *SAE Technical Papers* 2016; DOI:10.4271/2016-01-0718.
23. Singh R, Han T, Fatouraie M et al. Influence of fuel injection strategies on efficiency and particulate emissions of gasoline and ethanol blends in a turbocharged multi-cylinder direct injection engine *International Journal of Engine Research* 2021; 22(1):152–164; DOI:10.1177/1468087419838393.
24. Singh R, Morganti K and Dibble R. Optimizing split fuel injection strategies to avoid pre-ignition and super-knock in turbocharged engines. *International Journal of Engine Research* 2021; 22(1):199–221; DOI:10.1177/1468087419836591.
25. Okada Y, Miyashita S, Izumi Y et al. Study of Low-Speed Pre-Ignition in Boosted Spark Ignition Engine. *SAE International Journal of Engines* 2014; 7(2): 584–594. DOI: 10.4271/2014-01-1218.
26. Jatana GS, Splitter DA, Kaul B et al. Fuel property effects on low-speed pre-ignition. *Fuel* 2018; 230: 474–482. DOI: 10.1016/j.fuel.2018.05.060.
27. Amann M, Mehta D and Alger T. Engine Operating Condition and Gasoline Fuel Composition Effects on Low-Speed Pre-Ignition in High-Performance Spark Ignited Gasoline Engines. *SAE International Journal of Engines* 2011; 4(1): 274–285. DOI:10.4271/2011-01-0342.
28. Mansfield AB, Chapman E and Briscoe K. Effect of market variations in gasoline composition on aspects of stochastic pre-ignition. *Fuel* 2016; 184: 390–400. DOI:10.1016/j.fuel.2016.07.010.
29. Liu H, Wang Z, He X et al. Super-knock suppression for highly turbocharged gasoline engines using lean mixture control strategy with the same energy density. *International Journal of Engine Research* 2021; 22(2):665–673. DOI:10.1177/1468087419852839.
30. Takeuchi K, Fujimoto K, Hirano S, et al. Investigation of Engine Oil Effect on Abnormal Combustion in Turbocharged Direct Injection-Spark Ignition Engines. *SAE International Journal of Fuels and Lubricants* 2012; 5(3):1017–1024. DOI: 10.4271/2012-01-1615.
31. Hirano S, Yamashita M, Fujimoto K et al. Investigation of engine oil effect on abnormal combustion in turbocharged direct injection - Spark ignition engines (Part 2). *SAE Technical Papers* 2013; DOI:10.4271/2013-01-2569.
32. Welling O, Collings N, Williams J et al. Impact of lubricant composition on low-speed pre-ignition. *SAE Technical Papers* 2014; DOI:10.4271/2014-01-1213.
33. Fujimoto K, Yamashita M, Hirano S et al. Engine Oil Development for Preventing Pre-Ignition in Turbocharged Gasoline Engine. *SAE International Journal of Fuels and Lubricants* 2014; 7(3): 869–874. DOI:10.4271/2014-01-2785.
34. Onodera K, Kato T, Ogano S et al. Engine Oil Formulation Technology to Prevent Pre-ignition in Turbocharged Direct Injection Spark Ignition Engines. *SAE Technical Papers* 2015; DOI:10.4271/2015-01-2027.
35. Morikawa K, Moriyoshi Y, Kuboyama T, et al. Investigation of Lubricating Oil Properties Effect on Low Speed Pre-Ignition. *SAE Technical Papers* 2015; DOI:10.4271/2015-01-1870.
36. Ritchie A, Boese D and Young AW. Controlling Low-Speed Pre-Ignition in Modern Automotive Equipment Part 3: Identification of Key Additive Component Types and Other Lubricant Composition Effects on Low-Speed Pre-Ignition. *SAE International Journal of Engines* 2016; 9(2). DOI:10.4271/2016-01-0717.
37. Maharjan S, Qahtani Y, Roberts W, et al. The Effect of Pressure, Temperature and Additives on Droplet Ignition of Lubricant Oil and Its Surrogate. *SAE Technical Papers* 2018; DOI:10.4271/2018-01-1673.
38. Haas FM, Won SH, Dryer FL et al. Lube oil chemistry influences on autoignition as measured in an ignition quality

tester. *Proceedings of the Combustion Institute* 2019; 37(4): 4645–4654. DOI:10.1016/j.proci.2018.06.165.

39. Andrews A, Burns R, Dougherty R et al. Investigation of Engine Oil Base Stock Effects on Low Speed Pre-Ignition in a Turbocharged Direct Injection SI Engine. *SAE International Journal of Fuels and Lubricants* 2016; 9(2). DOI:10.4271/2016-01-9071.
40. Moriyoshi Y, Kuboyama T, Morikawa K, et al. A Study of Low Speed Preignition Mechanism in Highly Boosted SI Gasoline Engines. *SAE International Journal of Engines* 2016; 9(1):98–106. DOI:10.4271/2015-01-1865.
41. Ohtomo M, Suzuoki T, Miyagawa H et al. Fundamental analysis on auto-ignition condition of a lubricant oil droplet for understanding a mechanism of low-speed pre-ignition in highly charged spark-ignition engines. *International Journal of Engine Research* 2019; 20(3): 292–303. DOI:10.1177/1468087417751240.
42. Ullal A, Ra Y, Naber JD et al. Numerical investigation of oil droplet combustion using single particle ignition cell model. *International Journal of Engine Research* 2021; 22(5):1465–1483. DOI:10.1177/1468087419896939.
43. API. API 1509 Annex E - API Base Oil Interchangeability Guidelines for Passenger Car Motor Oils and Diesel Engine Oils, 2019.
44. ASTM International. Standard Test Method for Evaluation of Performance of Automotive Engine Oils in the Mitigation of Low-Speed , Preignition in the Sequence IX Gasoline Turbocharged Direct-Injection, Spark-Ignition Engine, 2020. DOI:10.1520/D8291-20.1.1.
45. Payri R, Viera JP, Pei Y et al. Experimental and numerical study of lift-off length and ignition delay of a two-component diesel surrogate. *Fuel* 2015; 158: 957–967. DOI:10.1016/j.fuel.2014.11.072.
46. Baert R, Frijters P, Somers B et al. Design and operation of a high pressure, high temperature cell for HD diesel spray diagnostics: guidelines and results. *SAE Technical Papers* 2009; DOI:10.4271/2009-01-0649.
47. Payri R, Gimeno J, Viera JP et al. Needle lift profile influence on the vapor phase penetration for a prototype diesel direct acting piezoelectric injector. *Fuel* 2013; 113: 257–265. DOI:10.1016/j.fuel.2013.05.057.
48. Payri R, Salvador FJ, Gimeno J et al. Flow regime effects over non-cavitating Diesel injection nozzles. *Proceedings of the Institution of Mechanical Engineers, Part D: Journal of Automobile Engineering* 2012; 226(1): 133–144. DOI:10.1177/0954407011413056.
49. Payri R, Tormos B, Salvador FJ et al. Spray droplet velocity characterization for convergent nozzles with three different diameters. *Fuel* 2008; 87(15-16): 3176–3182. DOI:10.1016/j.fuel.2008.05.028.
50. Payri R, Araneo L, Shakal JS et al. Phase doppler measurements: System set-up optimization for characterization of a diesel nozzle. *Journal of Mechanical Science and Technology* 2008; 22(8): 1620–1632. DOI:10.1007/s12206-008-0432-7.
51. Payri R, Salvador FJ, Gimeno J et al. Flow regime effects on non-cavitating injection nozzles over spray behavior. *International Journal of Heat and Fluid Flow* 2010; 32(1): 273–284.
52. Kuti OA, Yang SY, Hourani N et al. A fundamental investigation into the relationship between lubricant composition and fuel ignition quality. *Fuel* 2015; 160: 605–613. DOI:10.1016/j.fuel.2015.08.026.
53. API. API 1509 Engine Oil Licensing and Certification System, 2019.
54. ACEA. European Oil Sequences 2016 rev 3, 2020.
55. Payri R, Viera JP, Gopalakrishnan V et al. The effect of nozzle geometry over ignition delay and flame lift-off of reacting direct-injection sprays for three different fuels. *Fuel* 2017; 199: 76–90. DOI:10.1016/j.fuel.2017.02.075.
56. Yraguen BF, Poursadegh F and Genzale CL. Assessment of engine combustion network recommendations for measurement of ignition and lift-off length. *International Journal of Engine Research* 2020; (In press). DOI:10.1177/1468087420922646.
57. Engine Combustion Network (ECN), ecn.sandia.gov.
58. Fansler TD and Parrish SE. Spray measurement technology: a review. *Measurement Science and Technology* 2015; 26(1): 012002. DOI:10.1088/0957-0233/26/1/012002.
59. Bardi M, Payri R, Malbec LM et al. Engine Combustion Network: Comparison of Spray Development, Vaporization, and Combustion in Different Combustion Vessels. *Atomization and Sprays* 2012; 22(10): 807–842. DOI:10.1615/AtomizSpr.2013005837.
60. Benajes J, Payri R, Bardi M et al. Experimental characterization of diesel ignition and lift-off length using a single-hole ECN injector. *Applied Thermal Engineering* 2013; 58(1-2): 554–563. DOI:10.1016/j.applthermaleng.2013.04.044.
61. Lillo PM, Pickett LM, Persson H et al. Diesel Spray Ignition Detection and Spatial/Temporal Correction. *SAE Paper 2012-01-1239* 2012; : 1–21DOI:10.4271/2012-01-1239.
62. Pickett LM, Kook S and Williams TC. Visualization of Diesel Spray Penetration, Cool-Flame, Ignition, High- Temperature Combustion, and Soot Formation Using High-Speed Imaging. *SAE Int J Engines* 2009; 2(1): 439–459. DOI:10.4271/2009-01-0658.
63. Skeen SA, Manin J and Pickett LM. Simultaneous formaldehyde PLIF and high-speed schlieren imaging for ignition visualization in high-pressure spray flames. *Proceedings of the Combustion Institute* 2015; 35(3): 3167–3174. DOI:10.1016/j.proci.2014.06.040.
64. Desantes JM, Garcia-Oliver JM, Novella R et al. A numerical study of the effect of nozzle diameter on diesel combustion ignition and flame stabilization. *International Journal of Engine Research* 2020; 21(1): 101–121. DOI:10.1177/1468087419864203.
65. Siebers DL. Liquid-Phase Fuel Penetration in Diesel Sprays. *SAE Technical Paper 980809* 1998; : 1–23DOI:10.4271/980809.
66. Payri R, Salvador FJ, Bracho G et al. Differences between single and double-pass schlieren imaging on diesel vapor spray characteristics. *Applied Thermal Engineering* 2017; 125: 220–231. DOI:10.1016/j.applthermaleng.2017.06.140.
67. Won SH, Dooley S, Veloo PS et al. The combustion properties of 2,6,10-trimethyl dodecane and a chemical functional group analysis. *Combustion and Flame* 2014; 161(3): 826–834. DOI:10.1016/j.combustflame.2013.08.010.
68. Kassai M, Shiraishi T, Noda T et al. An Investigation on the Ignition Characteristics of Lubricant Component Containing Fuel Droplets Using Rapid Compression and Expansion Machine. *SAE International Journal of Fuels and Lubricants*

2016; 9(3): 469–480. DOI:10.4271/2016-01-2168.
69. Splitter D, Kaul B, Szybist J et al. Fuel-Lubricant Interactions on the Propensity for Stochastic Pre-Ignition. *SAE Technical Papers* 2019; DOI:10.4271/2019-24-0103.